

Enzymatic GTP Hydrolysis: Insights from an ab Initio Molecular Dynamics Study

Andrea Cavalli[†] and Paolo Carloni^{*‡}

Contribution from Scuola Internazionale Superiore di Studi Avanzati,
Istituto Nazionale di Fisica della Materia, Via Beirut 2-4, I-34014 Trieste, Italy

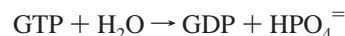
Received March 14, 2001

Abstract: Ab initio methods were used to shed light on fundamental aspects of the enzymatic mechanism of guanosine triphosphate hydrolysis in the Cdc42/Cdc42GAP complex. The calculations focused on the nucleophilic addition of the catalytic water molecule to the γ -phosphate phosphorus atom. A large model system was required to correctly reproduce the electrostatic properties on the active site. The model turned out to reproduce most of the electrostatic field of the biological complex at the reactants. Our calculations established the H-bond pattern of the catalytic water (WAT), which turned out to interact with Q61 and T35, in the most stable conformation. This ruled out the possibility that the catalytic water transferred its proton directly to the γ -phosphate. Furthermore, the calculations suggested that the electronic structure of WAT was very different from that in the bulk. Finally, this study showed that during the reaction, WAT transferred a proton to Gln61, consistent with the available X-ray data on a transition-state analogue/enzyme complex¹⁹ and with the decrease of activity in the Q61E mutant.⁶⁴

Introduction

Phosphoryl transfer reactions play a crucial role in widespread cellular functions, ranging from the signaling¹ and stress-activated² pathways to the biosynthesis of nucleic acids.³ The key step of action of (de)phosphorylating enzymes is the transfer of a phosphoryl group of adenosine or guanosine triphosphate (ATP and GTP, respectively) to acceptors such as water (hydrolases), amino acids residues (kinases), and other nucleotides (nucleoside monophosphate kinases). Within the family of hydrolases, the low molecular weight GTP-binding proteins (LMWGs⁴) hold a prominent position. They are central for a variety of biological processes including organization of the actin cytoskeleton,⁵ vesicular trafficking,⁶ cell cycle progression,⁷ control of transcription,^{8–12} and cell growth control.¹³

LMWGs use their intrinsic GTPase activity to act as molecular switches. Upon GTP binding, these proteins perform their functions ("on" state). Subsequently, GTP is hydrolyzed to GDP and the proteins become inactive ("off" state).¹⁴



This enzymatic activity can be highly enhanced by interacting with GTPase-activating proteins (GAPs).¹⁵

A vivid view of the interactions among GTP, the catalytic water, and the protein has been provided by a large number of high-resolution structures of complexes with transition-state analogues.¹⁶ These studies have pointed an extremely high structural similarity among the proteins belonging to the LMWG class.^{17,18} As an example, Figure 1a shows the structure of one member of this family, Cdc42/Cdc42GAP/GDP (PDB code 1GRN¹⁹), bound to AlF₃, which is an excellent transition-state mimic in phosphoryl transfer reactions.^{16,20,21}

On the basis of this structural information, different and conflicting proposals for the enzymatic mechanism have been

* To whom correspondence should be addressed. Address: International School for Advanced Studies, Via Beirut 4, I-34014 Trieste, Italy. Phone: +39-040-3787407. Fax: +39-040-3787528. E-mail: carloni@sissa.it.

[†] Current Address: Department of Pharmaceutical Sciences, University of Bologna, Via Belmeloro 6, I-40126 Bologna, Italy.

[‡] International Center for Genetic Engineering and Biotechnology, Padriciano 99, I-34012 Trieste, Italy.

- (1) Takai, Y.; Kishimoto, A.; Inoue, M.; Nishizuka, Y. *J. Biol. Chem.* **1977**, *252*, 7603–7609.
- (2) Kyriakis, J. M.; Avruch, J. *J. Biol. Chem.* **1996**, *271*, 24313–24316.
- (3) Koerner, J. F. *Annu. Rev. Biochem.* **1970**, *39*, 291–322.
- (4) Shinjo, K.; Koland, J. G.; Hart, M. J.; Narasimhan, V.; Johnson, D. I.; Evans, T.; Cerione, R. A. *Proc. Natl. Acad. Sci. U.S.A.* **1990**, *87*, 9853–9857.
- (5) MacKay, D. J. G.; Hall, A. *J. Biol. Chem.* **1998**, *273*, 20685–20688.
- (6) Wu, W.; Erickson, J. W.; Lin, R.; Cerione, R. A. *Nature* **2000**, *405*, 800–803.
- (7) Van Aelst, L.; D'Souza-Schorey, C. *Genes Dev.* **1997**, *11*, 2295–2322.
- (8) Coso, O. A.; Chiarielli, M.; Yu, J. C.; Teramoto, H.; Crespo, P.; Xu, N.; Miki, T.; Gutkind, J. S. *Cell* **1995**, *81*, 1137–1146.
- (9) Minden, A.; Lin, A.; Claret, F.-X.; Abo, A.; Karin, M. *Cell* **1995**, *81*, 1147–1157.
- (10) Olson, M. E.; Ashworth, A.; Hall, A. *Science* **1995**, *269*, 53–62.
- (11) Zhang, S.; Han, J.; Sells, N. A.; Chernoff, J.; Knaus, U. G.; Ulevitch, R. J.; Bokoch, G. M. *J. Biol. Chem.* **1995**, *270*, 23934–23936.

- (12) Bagrodia, S.; Derigard, B.; Davis, R. J.; Cerione, R. A. *J. Biol. Chem.* **1995**, *270*, 27995–27998.
- (13) Lin, R.; Bagrodia, S.; Cerione, R. A.; Manor, D. *Curr. Biol.* **1997**, *7*, 794–797.
- (14) Symson, M. *Trends Biochem. Sci.* **1996**, *21*, 178–181.
- (15) Lamarche, N.; Hall, A. *Trends Genet.* **1994**, *10*, 436–440.
- (16) Schlichting, I.; Reinstein, J. *Nat. Struct. Biol.* **1999**, *6*, 721–723.
- (17) de Vos, A. M.; Tong, L.; Milburn, M. V.; Matias, P. M.; Jancarik, J.; Noguchi, S.; Nishimura, S.; Miura, K.; Ohtsuka, E.; Kim, S. H. *Science* **1988**, *239*, 888–893.
- (18) Rittinger, K.; Walker, P. A.; Eccleston, J. F.; Nurmahomed, K.; Owen, D.; Laue, E.; Gamblin, S. J.; Smerdon, S. J. *Nature* **1997**, *388*, 683–697.
- (19) Nassar, N.; Hoffman, G. R.; Manor, D.; Clardy, J. C.; Cerione, R. A. *Nat. Struct. Biol.* **1998**, *5*, 1047–1052.
- (20) Wittinghofer, A. *Curr. Biol.* **1997**, *7*, 682–685.
- (21) Xu, Y.-X.; Morera, S.; Jonin, J.; Cherfils, J. *Proc. Natl. Acad. Sci. U.S.A.* **1997**, *94*, 3579–3583.

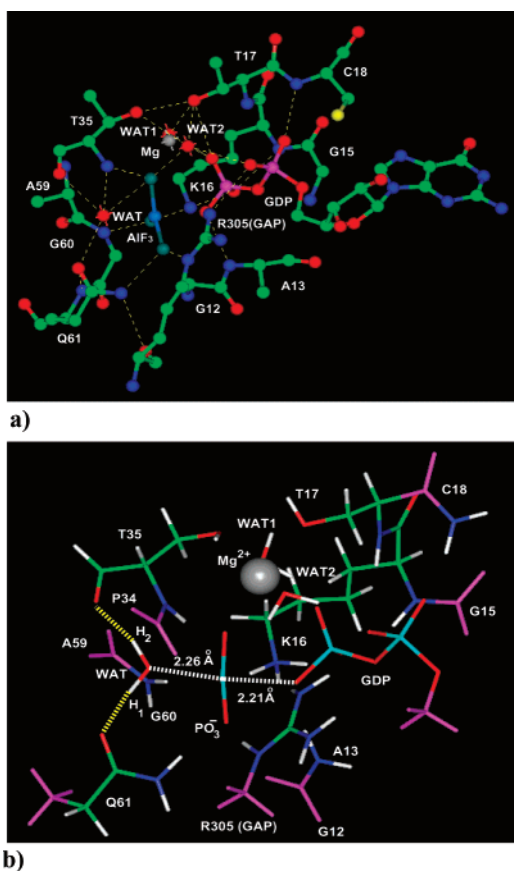


Figure 1. (a) X-ray structure of Cdc42 active site complexed with AlF_3 and GDP. Several positively charged groups (Mg^{2+} , Lys16, and GAP-Arg305) have a clear electrostatic role by stabilizing the negatively charged phosphate groups. This structure exhibits the complete Mg^{2+} coordination polyhedron; the cation is octahedrally coordinated by WAT1, WAT2, Thr35, Thr17, one oxygen from the β -phosphate, and one from the γ -phosphate. (b) Model system used in the quantum mechanical calculations. The following atoms were actually retained: the carbonyl groups of G12, G15, P34, and A59 to cap the amine of the following amino acids; the nitrogens of A13, C18, and G60 to cap the carbonyl of the preceding residues; all atoms from K16, T17, and T35; the side chain from Q61 and the methylguanidine from R305 of GAP; three water molecules (WAT, WAT1, WAT2, which correspond to HOH526, HOH527, HOH545, respectively, of the PDB file), Mg^{2+} cation; and GDP modeled as methyl diphosphate. The atoms kept fixed in the calculations are magenta. H bonds are yellow.

reported. These proposals differ in the description of two key steps of the reaction: (i) the formation of the highly nucleophilic agent OH^- and (ii) its binding to GTP with the formation of GDP and inorganic phosphate.

For step i, two different scenarios have been proposed. In one, Gln61 would act as a base toward the catalytic water molecule,^{22–24} thus accepting a proton before or during water nucleophilic attack. This proposal is consistent with the observation that a water molecule between Gln61 and GTP^{19,25} is perfectly positioned for a direct attack on the γ -phosphate and consistent with the fact that this residue is essential for the catalysis. However, the role of Gln61 as base has been questioned because of the large difference in pK_a between the

amide group of glutamine side chain and the catalytic water.²⁶ It has therefore been proposed that the substrate itself (γ -phosphate) would act as a base during the hydrolysis.

For step ii, either a dissociative²⁷ or an associative pathway²⁸ has been proposed.

Clearly, a quantum chemical description would be highly useful for discriminating between these different scenarios. Furthermore, it could shed light on site-directed mutagenesis experiments performed in the LMWG family. Finally, it might unravel the electronic properties of the catalytic water, highly polarized by the active-site residues.

Here, we have focused on step i of the reaction by using Car–Parrinello (CP)²⁹ density functional theory (DFT) molecular dynamics (MD) simulations. The DFT-MD approach has already been successfully applied to study the formation or breakup of chemical bonds,^{30,31} to study proton-transfer processes,^{32,33} and to describe enzymatic reactions.^{34–36}

The calculations were based on the crystal structure of the $\text{AlF}_3/\text{GDP}/\text{Cdc42GAP}/\text{Cdc42}$ complex¹⁹ (Figure 1), which provides a complete description of the essential Mg^{2+} coordination shell. Because of the crucial role of the entire preorganized active site for optimal interactions with the transition state,³⁷ our model (Figure 1b) consisted of all the residues interacting with GTP and the catalytic water molecule. Electrostatic calculations suggested that this model accounted for the major contribution of the protein electric field on the reactants, and yet, it was still manageable from a computational point of view. Our calculations provide further evidence of the postulated role of Gln61 as base during water nucleophilic attack. They show that the catalytic water molecule (WAT) is highly polarized by the active-site frame and it donates a proton to Gln61, whereas the proton transfer from WAT to γ -phosphate is geometrically, as well as energetically, highly unfavorable.

Methods

Quantum Chemical Calculations. Our model system was obtained from the X-ray structure of the $\text{AlF}_3/\text{GDP}/\text{Cdc42GAP}/\text{Cdc42}$ complex¹⁹ by substituting the AlF_3 moiety with the PO_3^- group (Figure 1b) and by adding hydrogen atoms, assuming standard bond lengths and angles. At the present stage, we cannot simulate the entire protein by ab initio methods. We considered a truncated model, which attempted to capture the physicochemical properties of substrate–enzyme interactions at the active site (Figure 1b). We included the chemical groups, which contributed more than 80% to the total electric field on the reactants, based on classical electrostatic modeling. The model took into account

- (22) Pai, E. F.; Kabsch, W.; Krengel, U.; Holmes, K.; John, J.; Wittinghofer, A. *Nature* **1989**, *341*, 209–214.
 (23) Pai, E. F.; Krengel, U.; Petsko, G. A.; Goody, R. S.; Kabsch, W.; Wittinghofer, A. *EMBO J.* **1990**, *9*, 2351–2359.
 (24) Krengel, U.; Schlichting, I.; Scherer, A.; Schumann, R.; Frech, M.; John, J.; Pai, E. F.; Wittinghofer, A. *Cell* **1990**, *62*, 539–548.
 (25) Scheffzek, K.; Ahmadian, M. R.; Kabsch, W.; Wiesmuller, L.; Lautwein, A.; Schmitz, F.; Wittinghofer, A. *Science* **1997**, *277*, 333–338.

- (26) Maegley, A. M.; Suzanne, J. A.; Herschlag, D. *Proc. Natl. Acad. Sci. U.S.A.* **1996**, *93*, 8160–8166.
 (27) Support to the dissociative mechanism is provided by FTIR data. Du, X.; Frei, H.; Kim, S.-H. *J. Biol. Chem.* **2000**, *275*, 8492–8500.
 (28) Support to the associative mechanism is given by the calculations of Florian and Warshel (Florian, J.; Warshel, A. *J. Phys. Chem. B* **1998**, *102*, 719–734.). Subsequent ab initio calculations by Futatsugi et al. (Futatsugi, N.; Hata, M.; Hoshino, T.; Tsuda, M. *Biophys. J.* **1999**, *77*, 3287–3292.), which provide further insight to GTP hydrolysis mechanism, have been subjected to serious criticism (Glennon, T. M.; Villa, J.; Warshel, A. *Biochemistry* **2000**, *39*, 9641–9651.).
 (29) Car, R.; Parrinello, M. *Phys. Rev. Lett.* **1985**, *55*, 2471–2474.
 (30) Röthlisberg, U.; Klein, M. L. *J. Am. Chem. Soc.* **1995**, *117*, 42–48.
 (31) Doclo, K.; Röthlisberg, U. *Chem. Phys. Lett.* **1995**, *297*, 205–210.
 (32) De Santis, L.; Carloni, P. *Proteins: Struct., Funct., Genet.* **1999**, *37*, 611–618.
 (33) Piana, S.; Carloni, P. *Proteins: Struct., Funct., Genet.* **2000**, *39*, 26–36.
 (34) Röthlisberg, U.; Carloni, P. *Int. J. Quantum Chem.* **1999**, *73*, 209–218.
 (35) Rovira, C.; Carloni, P.; Parrinello, M. *J. Phys. Chem. B* **1999**, *103*, 7031–7035.
 (36) Alber, F.; Carloni, P. *Protein Sci.* **2000**, *9*, 2535–2546.
 (37) Warshel, A. *J. Biol. Chem.* **1998**, *273*, 27035–27038.

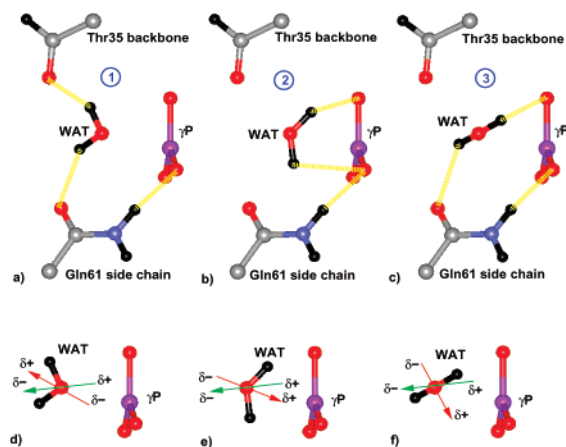


Figure 2. Orientation of WAT in the catalytic cavity. In **1** (a), WAT H-bonds to the Thr35 backbone and Gln61 side chain carbonyl oxygens. In **2** (b), WAT H-bonds to the γ -phosphate group. In **3** (c), WAT H-bonds to γ -phosphate and the Gln61 side chain. Ab initio calculations showed that **1** was more stable than **2** by ~ 65 kcal/mol. Interactions between WAT dipole moment (red) and the protein electric field (green) in **1**, **2**, and **3** are shown in parts d, e, and f, respectively. In parts a–c H bonds are depicted in yellow.

all the substrate–enzyme interactions, while it was still manageable from a computational point of view. Its overall charge turned out to be zero. WAT hydrogen atoms were positioned in three plausible conformations, which resulted in as many different H-bond patterns (Figure 2a–c). Ab initio geometry optimizations and classical modeling (see Results) identified **1** (Figure 2a) as the most stable conformer, and all subsequent calculations were carried out with this H-bond pattern.

The quantum problem was solved within the DFT framework. Gradient-corrected exchange and correlation functionals with Becke³⁸ and Lee–Yang–Parr³⁹ (BLYP) parametrizations were used. The interactions between the ionic cores and valence electrons were described by Martins–Truollier type pseudopotentials.⁴⁰ The Kohn–Sham orbitals were expanded in plane waves up to 70 Ry ($\sim 200\,000$ basis functions). The complex was treated like an isolated system.⁴¹ Geometry optimizations were performed using the direct inversion in the iterative subspace (DIIS) method^{42,43} until a convergence of 0.0005 au on the gradients was reached. Ab initio molecular dynamics (ab initio MD) simulations were performed following the Car–Parrinello scheme.²⁹ The positions of the formyl groups of G12, G15, C18, P34, and A59, and the methyl groups of the methyl triphosphate, the methylguanidinium, and the propionamide were kept fixed to mimic the presence of the protein frame (Figure 1b), following the procedure of ref 36. A time step of 0.121 fs and a fictitious electron mass of 500 au were used. (The time step used has been reported also for other hydrogen-containing systems.^{44,45}) The system was coupled to a Nosé–Hoover thermostat⁴⁶ of 500 cm^{-1} frequency in order to maintain the temperature at 300 K. The size cell was set large enough so that the electron density decayed to zero within the simulation box ($18.7 \times 17.3 \times 18.6 \text{ \AA}^3$). The ab initio MD simulations were done by using the parallel version of the Car–Parrinello code (CPMD, version 3.3⁴⁷).

During the constrained ab initio MD simulations, the constraint force (CF) on the reaction coordinate ($O_{\text{W}}-\gamma\text{P}$ distance) was monitored in order to qualitatively detect the stability of the transition state. A positive value of CF corresponds to a repulsive force. This implied that the $O_{\text{W}}-\gamma\text{P}$ bond would have been disrupted if the constraint had been removed.

A negative value of CF, which corresponds to an attractive force, implied the formation of the $O_{\text{W}}-\gamma\text{P}$ bond upon removal of the constraint and the evolution of the system toward the products. Each constrained MD run was carried out for ~ 0.5 ps, which is considerably less than the time scale required to quantitatively estimate the free energy. However, in our study we were interested in the structural and qualitative aspects of the phosphoryl transfer reactions. To this aim, we used constrained dynamics only to build up structural models by decreasing the $O_{\text{W}}/\gamma\text{P}$ distance.

Since in the ultrashort time scale explored the constraint force might be excessively large, we performed a test calculation by prolonging the ab initio MD run at $d = 2.2 \text{ \AA}$ by 1 ps. The constraint force turned out to be rather stable after changing its sign, suggesting that the time scale used was adequate to describe qualitative aspects of the reaction.

Test calculations were also carried out on the model system of Figure 1b, in which the catalytic water molecule (WAT) was replaced by OH^- anion. The $O_{\text{W}}/\gamma\text{P}$ distance was set at a crystal structure value of 2.26 \AA . A total of 0.4 ps of ab initio MD simulations at room temperature were performed.

All calculations required approximately 60 000 CPU hours on a Cray T3E machine.

Calculated Properties. As the system evolved, the following properties were calculated from room-temperature selected snapshots of the ab initio MD.

(i) The chemical bonding was characterized in terms of maximally localized Wannier orbital centers (WOCs).^{48–51} WOCs were also calculated taking into account the classical electrostatic field due to the protein frame and then used to estimate the catalytic water (WAT) dipole moment,

$$\vec{\mu} = -2e \sum_{i=1}^{N/2} \vec{r}_i + e \sum_I Z_I \vec{R}_I$$

as reported in ref 51. This allowed us to make a comparison of WAT dipole moments in three different cases: (a) in the electric field generated by the active site atoms, (b) in the field generated by the entire protein, and (c) in water solution.⁵¹ Shifts of WOCs along the chemical bond correlate to differences of Pauling electronegativities between the atoms forming the bond.⁵² As in ref 53, the WOCs analysis was used to investigate the changes of polarity upon formation of the intermolecular complexes.

(ii) Analysis based on the electron localization function (ELF) was also performed^{54–56} to characterize the nature of a low-barrier hydrogen bond. ELF has been shown to be a useful tool in studying the nature of the chemical bond.^{32,57} In particular, ELF red areas indicate strong electron localization such as spatial regions where the Pauli principle has little influence on the electron distribution.

Classical Electrostatic Modeling. The electric field of the entire protein, immersed in a water box with periodic boundary conditions,

(38) Becke, A. D. *Phys. Rev. A* **1988**, *38*, 3098–3100.

(39) Lee, C.; Yang, W.; Parr, R. C. *Phys. Rev. A* **1988**, *37*, 785–789.

(40) Troullier, N.; Martins, J. L. *Phys. Rev. B* **1991**, *43*, 1993–2006.

(41) Barnett, R. N.; Landmann, U. *Phys. Rev. B* **1993**, *48*, 2081–2097.

(42) Pulay, P. *Chem. Phys. Lett.* **1980**, *73*, 393–398.

(43) Hutter, J.; Lüthi, H. P.; Parrinello, M. *Comput. Mater. Sci.* **1994**, *2*, 244–248.

(44) Molteni, C.; Parrinello, M. *J. Am. Chem. Soc.* **1998**, *120*, 2168–2171.

(45) Doclo, K.; Röthlisberg, U. *J. Phys. Chem. A* **2000**, *104*, 6464–6469.

(46) Nosé, S. *J. Chem. Phys.* **1984**, *81*, 511–519.

(47) Hutter, J.; Ballone, P.; Bernasconi, M.; Focher, P.; Fois, E.; Goedecker, S.; Parrinello, M.; Tuckerman, M. *CPMD 3.3*; MPI für Festkör-Perforforschung and IBM Zürich Research Laboratory: Zurich, Switzerland, 1999.

(48) Silvestrelli, P. L.; Marzari, N.; Vanderbilt, D.; Parrinello, M. *Solid State Commun.* **1998**, *107*, 7–11.

(49) Marzari, N.; Vanderbilt, D. *Phys. Rev. B* **1997**, *56*, 12847–12864.

(50) Vanderbilt, D.; King-Smith, R. D. *Phys. Rev. B* **1993**, *48*, 4442–4455.

(51) Silvestrelli, P. L.; Parrinello, M. *Phys. Rev. Lett.* **1999**, *82*, 3308–3311.

(52) Alber, F.; Folkers, G.; Carloni, P. *J. Chem. Phys. B* **1999**, *103*, 6121–6126.

(53) Sulpizi, M.; Carloni, P. *J. Chem. Phys. B* **2000**, *104*, 10087–10091.

(54) Becke, A. D.; Edgecombe, K. E. *J. Phys. Chem.* **1990**, *92*, 5397–5403.

(55) Silvi, B.; Savin, A. *Nature* **1994**, *371*, 683–686.

(56) Savin, A.; Nesper, R.; Wengert, S.; Fässler, T. F. *Angew. Chem., Int. Ed. Engl.* **1997**, *36*, 1808–1832.

(57) Schiott, B.; Iversen, B. B.; Madsen, G. K. H.; Larsen, F. K.; Bruice, T. C. *Proc. Natl. Acad. Sci. U.S.A.* **1998**, *95*, 12799–12802.

was calculated with a simple point charge model, based on the all-atom AMBER⁵⁸ force field. The field at position \vec{r}_0 then reads

$$\vec{E}(\vec{r}_0) = \frac{1}{4\pi\epsilon_0} \sum_i \frac{q_i}{r_{i0}^3} \vec{r}_{i0}$$

where the sum is performed on all the atoms in the system, q_i represents the charge of atom i , and \vec{r}_{i0} is the distance from \vec{r}_0 . The dielectric constant ϵ_0 is assumed to be equal to 1. The error due to the neglect of the contribution of the periodic images was estimated to be less than 5%. To build the model of the protein/water system, we used classical molecular dynamics simulations (see Supporting Information). Some calculations were carried out, including the electric field of the protein immersed in water.

Results

In this section, we investigated first the polarization effects and then the dynamics of the model depicted in Figure 1b. Subsequently, we explored the enzymatic reaction by performing constrained ab initio molecular dynamics simulations.

Cdc42/WAT/GTP Structural Model. Classical electrostatic calculations suggested that the model in Figure 1b generated as much as ~85% of the total protein electric field on reactants, the catalytic water (WAT), and the GTP. Consistently, ab initio electronic structure calculations showed that the dipole moment of WAT in the field of these residues was very similar to that in the presence of the entire enzymatic complex (3.86 and 3.80 D, respectively). Thus, we concluded that the model system of Figure 1b provided a good description of the electrostatically preorganized active site for the enzymatic catalysis.

Orientation of the Catalytic Water. In principle WAT can form several plausible H-bond patterns. It may H-bond to the Thr35 backbone and to the Gln61 side chain carbonyl oxygens (**1**, Figure 2a), to γ -phosphate oxygens (**2**, Figure 2b) or to Gln61 side chain, and to γ -phosphate (**3**, Figure 2c). Calculations on our model system (Figure 1b) suggested that conformer **1** was more stable by several tens of kcal/mol than **2**, which in turn was more stable than **3**. Environmental effects further stabilize conformation **1** relative to **2** and **3**. Indeed, the electric field of the protein was aligned to the calculated WAT dipole in conformer **1** (Figure 2d). In contrast, **2** and **3** were highly unstable with respect to the electric field generated by the enzymatic complex (Figure 2e,f). Thus, our quantum chemical calculations and classical electrostatic modeling provided a consistent picture in which WAT was oriented as in conformation **1**. Therefore, all subsequent calculations were carried out on this conformer.

In this conformation, WAT was highly polarized. Its dipole moment of 3.86 D was much larger than that of water in the bulk (3.00 D⁵¹).

Enzymatic Reaction. Ab initio MD simulations showed that the system was intrinsically unstable, since the complex turned out to decompose spontaneously during the dynamics to form the reactants. After a few hundred femtoseconds, the γ P–O(GDP) bond was formed and GTP and WAT (i.e., the reactants) were produced. Figure 3a shows a snapshot after ~0.2 ps of ab initio MD: the GTP is stabilized in the enzyme active site by electrostatic interactions with Mg²⁺, Lys16, and GAP/Arg305 (Figure 3b). WAT is 3.5 Å apart from the γ -phosphorus, and it maintained the H-bond pattern with both Gln61 and Thr35.

Because of the instability of the system toward the reactants, we decided to use constrained ab initio molecular dynamics⁵⁹ simulations to follow WAT nucleophilic attack to GTP. Specifically, we constrained the O_W/ γ P distance ($d(\text{O}_W/\gamma\text{P})$) as the reaction coordinate. Its value, which is 2.26 Å in the crystal structure, was shortened stepwise by 0.1 Å until 1.8 Å was reached. The evolutions of the GTP/WAT adduct toward the reactants or the products were detected by monitoring the

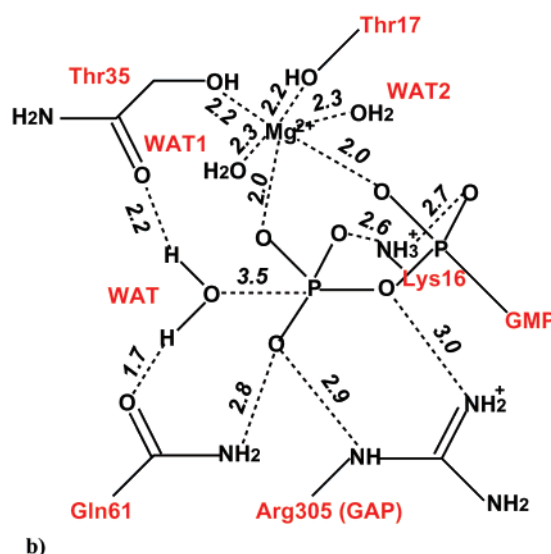
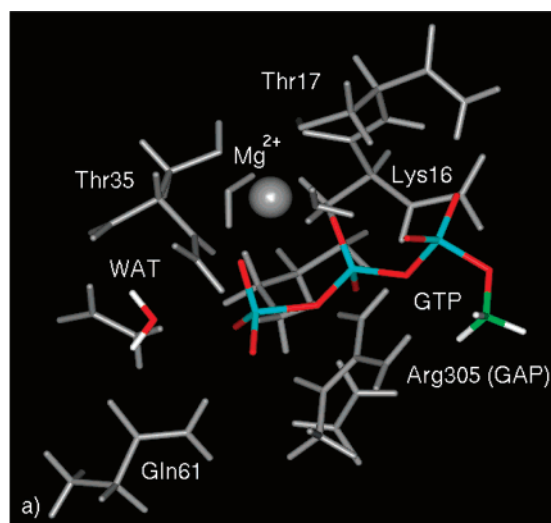


Figure 3. Ab initio MD of the model represented in Figure 1b. (a) After 0.21 ps, the reactants are formed. WAT is at 3.5 Å from the γ -phosphorus, and it maintained the H-bond pattern with both Gln61 and Thr35. (b) Selected intermolecular distances in the active site are presented (values are in Å).

constraint force (CF) values (see Methods). For $d(\text{O}_W/\gamma\text{P})$ between 2.2 and 1.9 Å, the CF values became negative (i.e., the O_W– γ P bond was formed) within 0.5 ps of simulations. However, upon removal of the constraints, the GTP/WAT complexes again evolved back to the reactants in a few hundred femtoseconds, possibly as a result of the adduct being unstable with respect to the reagents. For $d(\text{O}_W/\gamma\text{P}) = 1.8$ Å, WAT spontaneously transferred a proton to the carbonyl oxygen of the Gln61 side chain (O_{Gln61}) before CF became negative. In this case, removal of the constraint caused the spontaneous evolution of the system toward the products (Figure 4), which turned out to be stable for more than 1 ps of ab initio MD simulations. Similar results were obtained by replacing WAT of Figure 1b with OH[−]. By the positioning of the hydroxyl anion at the crystallographic position of 2.26 Å from the γ -phosphate phosphorus, the reaction products (i.e., GDP and inorganic phosphate) were formed after a few hundred femtoseconds of unconstrained ab initio MD. Thus, the highly nucleophilic species OH[−] appears to react very readily with the GTP in the active site of the enzyme. To confirm the formation of the new covalent bond, calculations of the electronic structure in terms of Kohn–Sham levels were carried out. This allowed the identification of a molecular orbital involving O_W and γ P, which provided striking evidence of the newly formed covalent bond O_W– γ P (Figure 4a).

(58) Cornell, W. D.; Cieplack, P.; Bayly, C. I.; Gould, I. R.; Merz, K. M.; Ferguson, D. M.; Spellmeyer, D. C.; Fox, T.; Kollman, P. A. *J. Am. Chem. Soc.* **1995**, *117*, 5179–5197.

(59) Carloni, P.; Sprick, M.; Andreoni, W. *J. Phys. Chem. B* **2000**, *104*, 823–835.

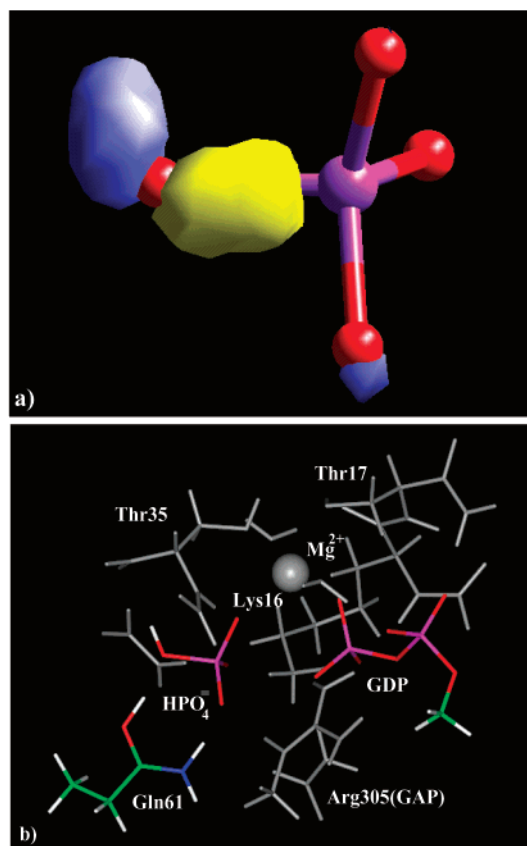


Figure 4. (a) Kohn–Sham one-electron molecular orbital. In yellow and blue are represented the positive and negative isodensity surfaces, respectively (± 15 au). (b) Products of GTP hydrolysis: GDP, HPO_4^{2-} , and the protonated form of Gln61.

Table 1. Distances (\AA) between O_W , O_{Gln61} , and WOCs during the Constrained *ab Initio* Molecular Dynamics Simulations^a

$d(\text{O}_W/\gamma\text{P})$	CF > 0			CF < 0		
	$\text{O}_{\text{Gln61}}\text{-a}$	$\text{O}_W\text{-b}$	$\text{O}_W\text{-c}$	$\text{O}_{\text{Gln61}}\text{-a}$	$\text{O}_W\text{-b}$	$\text{O}_W\text{-c}$
2.2	0.34	0.49	0.35	0.34	0.48	0.41
2.1	0.37	0.47	0.43	0.36	0.48	0.40
2.0	0.36	0.48	0.43	0.36	0.48	0.41
1.9	0.37	0.48	0.45	0.40	0.44	0.47
1.8	0.40	0.43	0.45	0.47	0.41	0.55

^a CF is either positive or negative. a represents WOC of the O_{Gln61} lone pair in the direction of H1. b represents WOC of the $\text{O}_W\text{-H1}$ bond. c represents WOC of the O_W lone pair in the direction of γP . When $d(\text{O}_W/\gamma\text{P}) = 1.8 \text{ \AA}$ and $\text{CF} < 0$, the system spontaneously evolved toward the products. The great displacements (in bold) observed when both $\text{CF} < 0$ and $d(\text{O}_W/\gamma\text{P}) = 1.8 \text{ \AA}$ can be a further clue for the newly formed covalent bond.

During the enzymatic reaction, the polarization effects were estimated by analyzing the displacements of the centers of maximally localized Wannier orbitals (WOCs) (Table 1). These orbitals, which correspond to the Boys orbitals of quantum chemistry,⁶⁰ provide a useful representation of electron lone pairs and chemical bond. Table 1 shows WOCs during the movement of WAT along the reaction coordinate. In particular, Table 1 shows that WAT O–H bonds were highly

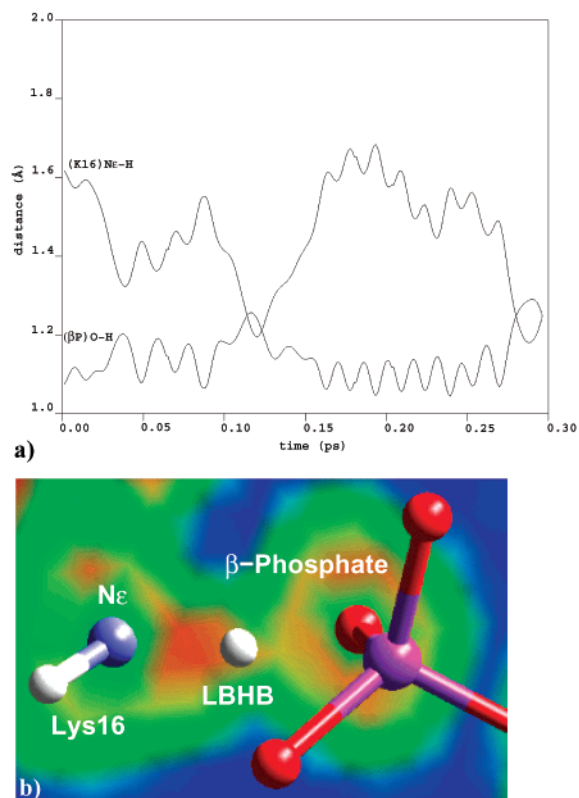


Figure 5. LBHB between β -phosphate and Lys16. (a) Plot of the relative distances between $(\text{Lys16})\text{Ne-H}$ and $(\beta\text{-phosphate})\text{O-H}$. Data are from the MD simulation at $d(\text{O}_W/\gamma\text{P}) = 1.8 \text{ \AA}$. (b) ELF from a single snapshot of MD simulation at $d(\text{O}_W/\gamma\text{P}) = 1.8 \text{ \AA}$. The ELF is projected on the plane containing $\text{O}(\beta\text{phosphate})$, H, and $\text{Ne}(\text{Lys16})$. ELF ranges are from blue (0.20) to red (0.98).

polarized and that the polarization effects were greatly increased by shortening the $\text{O}_W/\gamma\text{P}$ distance. Moreover, at $d(\text{O}_W/\gamma\text{P}) = 1.8 \text{ \AA}$, one of the O_W lone pairs was located on the $\text{O}_W\text{-}\gamma\text{P}$, confirming the formation of a new oxygen–phosphorus covalent bond.

In all simulations, it was also noticed that a proton hopping between Lys16 and the β -phosphate group occurred in the subpicosecond time scale. It happened when the distance between $\text{O}(\beta\text{-phosphate})$ and $\text{Ne}(\text{Lys16})$ was about 2.4 \AA . A plot of the $\text{Ne}(\text{K16})\text{-H}$ and $\text{O}(\beta\text{P})\text{-H}$ relative distances is shown in Figure 5a, confirming a proton transfer between these two groups. The chemical bonding of this interaction, referred in the literature as a low-barrier hydrogen bond (LBHB),^{61–63} was investigated by estimating the electron localization function (ELF)^{54–56} (Figure 5b). The plot was obtained by projecting ELF on the plane containing $\text{O}(\beta\text{P})$, H, and $\text{Ne}(\text{Lys16})$. Strong electronic localization was found between the phosphate and lysine, suggesting that the character of this LBHB was partly covalent, in agreement with a previous finding.³⁶

Discussion

We have presented here an *ab initio* quantum chemical study on the Cdc42/Cdc42GAP active site. Our goal was to investigate the initial and fundamental step of the enzymatic GTP hydrolysis, namely, the deprotonation of the catalytic water molecule (WAT).

A preliminary investigation was required to establish the reliability of the structural model and the critical orientation of

(60) Boys, S. F. *Proc. R. Soc.* **1950**, A200, 542.

(61) Cleland, W. W. *Biochemistry* **1992**, 31, 317–319.

(62) Cleland, W. W.; Kreevoy, M. M. *Science* **1995**, 264, 1887–1890.

(63) Sirois, S.; Proynov, E. I.; Nguyen, D. T.; Salahub, D. R. *J. Chem. Phys.* **1997**, 107, 6770–6781.

WAT in the active site. The relatively large model used, which included all the interactions between the triphosphate moiety and the enzyme active-site residues (Figure 1b), accounted for most of the protein electric field. Indeed, classical modeling suggested that the atoms in the active site accounted for as much as 85% of total protein electric field on the reactants. Besides, our quantum chemical calculations suggested that the WAT dipole moment in our model system did not vary significantly in the presence of the electric field of the protein frame. We could therefore conclude that our model system was able to account for the most relevant physicochemical features of the enzyme active site. WAT orientation as in **1** (Figure 2a), in which the catalytic water molecule forms H-bond interactions with Thr35 backbone and Gln61 side chain, was by far the most stable conformation. Furthermore, it was also highly stabilized by the electrostatic field generated by the entire enzymatic complex, which was in striking alignment with the dipole moment of WAT (Figure 2d–f). (WAT was more polarized in the protein than in bulk water. This may be consistent with the proposal that enzyme cavities act as a supersolvent.³⁷) This ruled out the possibility that the catalytic water transferred its proton directly to γ -phosphate, as previously suggested.²⁶ (Consistently, during the dynamics simulations WAT was never oriented to form H-bonds to γ -phosphate as in **2** or in **3** of Figure 2. Indeed, the angles between the WAT O–H bonds and γ -phosphate oxygens were always less than 95°.)

GTP enzymatic hydrolysis was investigated by carrying out ab initio MD on the model of Figure 1b. Because the system decomposed spontaneously during the dynamics to form the reactants (Figure 3), we subsequently used constrained ab initio MD.

The formation of the products was observed during the constraint dynamics at $d(\text{O}_w/\gamma\text{P}) = 1.8 \text{ \AA}$. The key step of the reaction was the proton transfer from WAT to the Gln61 side chain. This process stabilized the highly nucleophilic species OH^- , which could complete the nucleophilic attack to the GTP. This finding is consistent with the X-ray structure of the Cdc42-TS mimic complex,¹⁹ which clearly shows that NH_2 of the Gln61 side chain H-bonds to the γ -phosphate, maintaining Gln61 very close to the catalytic water molecule (Figure 1a), and might also offer an explanation for the 60–80% decrease in activity of the Q61E mutant.⁶⁴ Indeed, although Glu is a base stronger than Gln, it is expected to be located more apart from the catalytic water than Gln because of electrostatic repulsions between the carboxylate group of Glu and the triphosphate moiety of GTP.

A comment is about the reliability of our model for describing this proton-transfer event. Although the difference in pK_a 's between water and Gln61 in aqueous solution is very large,²⁶ our calculations showed that the WAT O–H bond, pointing toward Gln61, was highly polar, as shown by the displacements of Wannier orbital centers (Table 1). In particular, the difference in Pauling electronegativity between oxygen and hydrogen, estimated on the basis of the Wannier centers⁵² (see Methods), passed from 1.25 in isolated water⁵¹ to as much as 1.58 in our model system. The high polarity of the O–H bond is possibly due to the interaction of WAT oxygen with the highly electrophilic species γ -phosphorus, whose electron deficiency

may be greatly enhanced by the positively charged residues that compose the active site (i.e., Mg^{2+} and GAP/Arg305). Thus, because of the high polarity of the O–H bond, the catalytic water molecule, strongly interacting with the γ -phosphate phosphorous, may be able to protonate even a very weak base such as the amide group of Gln61 side chain. However, these calculations do not rule out the possibility of a proton transfer between WAT and the solvent, before reaching its reactive conformation. Actually, test calculations, using the OH^- anion instead of WAT, indeed showed that the reaction readily occurred in the catalytic site.

In addition, during the simulations a low-barrier hydrogen bond (LBHB) between Lys16 and β -phosphate was detected (Figure 5). This LBHB turned out to be partly covalent in nature, in agreement with a previous proposal.³⁶ The LBHB could in principle be very important for stabilizing the transition state, since it may provide a very large stabilization energy.^{61,62} Furthermore, it could enhance the water nucleophilic attack by reducing significantly the electron density on the β -phosphate and consequently increasing the γ -phosphate electrophilic power. However, such an interaction might arise from our calculations as a consequence of the truncations performed in the model and by the use of the BLYP approximation,⁶³ and thus, it cannot be firmly established by this work.

Conclusions

Water nucleophilic attack on GTP in the Cdc42/Cdc42GAP enzymatic complex was investigated by using ab initio molecular dynamics studies. The model system allowed us to consider the most relevant physicochemical interactions among GTP, the catalytic water molecule (WAT), and the biological complex. In particular, the system appeared to include the atoms forming the pre-organized catalytic site, and it accounted for the major contribution of the protein electric field on the reactants.

Quantum chemical and classical calculations suggested that the catalytic water H-bonds to Gln61 and Thr35 during its nucleophilic attack. Our calculations provided no evidence for the postulated proton transfer from WAT to the γ -phosphate. Instead, the highly nucleophilic species OH^- could be stabilized by a proton transfer to Gln61. This key event was accompanied by the formation of a low-barrier hydrogen bond between Lys16 and β -phosphate. During the constraint dynamics at $d(\text{O}_w/\gamma\text{P}) = 1.8 \text{ \AA}$, a chemical bond between γ -phosphorus and WAT oxygen was formed. In this simulation, removal of the constraint caused the spontaneous evolution of the system toward the products (i.e., GDP and inorganic phosphate). The products turned out to be stable for the rest of the simulation. These findings are fully consistent with X-ray data on the transition-state analogue complex^{17,19} and on site-directed mutagenesis data on the Q61E mutant.⁶⁴

Acknowledgment. This work was funded by the INFN project and the calculations were performed at CINECA in Bologna, Italy. We thank Maurizio Recanatini for the critical reading of the manuscript and Ugo Tartaglino for useful discussions.

Supporting Information Available: Details of the molecular dynamics simulations for the protein/water system (PDF). This material is available free of charge via the Internet at <http://pubs.acs.org>.

(64) Lerm, M.; Selzer, J.; Hoffmeyer, A.; Rapp, U. R.; Aktories, K.; Schmidt, G. *Infect. Immun.* **1999**, *67*, 496–503.